*Sensors and Materials*, Vol. 37, No. 3 (2025) 821–829
MYU Tokyo



S & M 3959

# Performance of Dye-sensitized Solar Cells Using Titanium Dioxide and Silver Nanowire Composite Film

Wei-Ling Hsu,[1] Tian-Chiuan Wu,[2*] Tung-Lung Wu,[3]
Kao-Wei Min,[4] Yu-Yang Tseng,[2] and Teen-Hang Meen[2**]

[1]School of Civil Engineering, Jiaying University, No. 100, Meisong Road,
Meijiang District, Meizhou City, Guangdong 514015, China
[2]Department of Electronic Engineering, National Formosa University, Huwei, Yunlin 632, Taiwan
[3]Department of Electrical Engineering, Lunghwa University of Science and Technology,
Guishan District, Taoyuan City 333, Taiwan
[4]Department of Electronic Engineering, Lunghwa University of Science and Technology,
Guishan District, Taoyuan City 333, Taiwan

(Received August 5, 2024; accepted February 19, 2025)

***Keywords:*** dye-sensitized solar cells, doctor blade method, titanium dioxide, AgNWs, molding

In this study, various concentrations of silver nanowires (AgNWs) were added to titanium dioxide ($TiO_2$) paste, which was then uniformly coated onto indium tin oxide (ITO) conductive glass substrates by a doctor blade method. The coated substrate underwent a molding process to ensure an average film thickness of 10 μm. Subsequently, the substrate was annealed in a high-temperature furnace to enhance the structural stability and electrical performance of dye-sensitized solar cells (DSSCs). After annealing, DSSCs were assembled with a photoanode, a thermoplastic film, and a counter electrode by a sandwich stacking method. The short-circuit current density ($J_{sc}$) and photovoltaic conversion efficiency (PCE) of the assembled DSSCs with various concentrations of AgNWs were measured. The DSSC without AgNWs presented a $J_{sc}$ of 7.71 mA/cm$^2$ and a PCE of 3.54%. In contrast, the DSSC with 0.05 wt% AgNWs exhibited an increased $J_{sc}$ of 8.14 mA/cm$^2$ and a PCE of 4.14%, representing a significant efficiency improvement.

## 1. Introduction

The development of dye-sensitized solar cells (DSSCs) began in 1976 when Japanese researchers H. Tsubomura and M. Matsumura invented the use of porous zinc oxide as the working electrode for DSSCs, achieving a power conversion efficiency of 2.5%. The DSSC has been improved and is regarded as a low-cost photovoltaic cell since the adoption of a mesoporous titanium dioxide ($TiO_2$) nanoparticle film as the electrode. Using the $TiO_2$ film also significantly increases the electrode's specific surface area. Such an increased surface area enables the efficient adsorption of the ruthenium-based dye onto the $TiO_2$ film. The DSSC is fabricated with

*Corresponding author: e-mail: eetcwu@nfu.edu.tw
**Corresponding author: e-mail: thmeen@gs.nfu.edu.tw
https://doi.org/10.18494/SAM5283

ISSN 0914-4935 
https://myukk.org/

the ruthenium-based dye and iodine/iodide ($I^-/I_3^-$) electrolyte, which enhances the photovoltaic conversion efficiency (PCE) from 7.1 to 8%.(1)

The DSSC presented a new direction for solar cell research and development as it requires low manufacturing costs but shows improved simplicity and stability. The advantages of the DSSC, such as reduced dependence on sunlight angles and high temperatures, along with its enhanced transparency and flexibility, make it widely used for indoor applications. These features also contribute to its vast market potential and its promise as a leading technology in the green energy industry.

In general, the DSSC consists of a glass substrate, a photoanode layer, and a platinum-coated counter electrode. $TiO_2$ is primarily used in the DSSC because of its nontoxicity, high chemical stability, strong oxidation capability, and low cost. The simplicity of the fabrication process contributes to the enhancement of the performance of the DSSC with composite materials. $TiO_2$ is an n-type semiconductor that excites electrons from the valence to the conduction band, forming electron–hole pairs under sufficient light. However, $TiO_2$ has a bandgap of 3.2 eV, thereby requiring ultraviolet (UV) light to generate electron–hole pairs. Such a property of $TiO_2$ necessitates extensive research to increase its photocatalytic activity and absorption of visible light.

The DSSC is a highly efficient photovoltaic device well-suited for powering small electronic applications under indoor light conditions such as wireless sensors for IoT and wireless networks.(2) The high efficiency of DSSCs makes them ideal for effectively harvesting power from ambient indoor light, providing a reliable and sustainable energy solution for energy autonomy and prolonged operation of wireless sensors.(3) The DSSC can also be applied in various sensor technologies. Rahmadwati *et al.* designed an optical sensor that uses power converted from ambient light using DSSCs consisting of photo-electrodes and $TiO_2$ photo-catalysts extracted from tobacco chlorophyll dye. The DSSCs in the optical sensor demonstrated versatility and potential in a wide range of applications, highlighting their role in the development of advanced sensing technologies.(4)

DSSCs present an efficient photovoltaic technology for powering various electronic applications and offer promising solutions for economical indoor photovoltaics that are thin, lightweight, and flexible. With low fabrication costs and abundant materials available for manufacturing, DSSCs are a highly attractive option in the green energy sector.(5) Aslam *et al.* highlighted the applications and addressed the challenges in using DSSCs for IoT applications.(6) To enhance PSE, silver nanomaterials are employed owing to localized surface plasmon resonance (LSPR), which is induced by the shape, size, and thickness of the nanostructure.(7) When light at a specific wavelength irradiates a metallic surface or metallic nanostructures, LSPR occurs, generating an electromagnetic field that decays exponentially from the surface into the surrounding medium. In this decaying wave, emitted photons are effectively concentrated, exciting the molecules of silver. This mechanism enhances the quantum yield, thereby improving PSE.(8)

On the basis of previous research results and the mechanism of improving the PCE of solar cells, we experimented with DSSCs fabricated with various concentrations of silver nanowires (AgNWs) and investigated the effect of AgNWs on the PCE of the DSSCs. The result provides a reference for further development of the DSSCs.

## 2. Materials and Methods

### 2.1 DSSC fabrication

We fabricated DSSCs that have a sandwich-like stacking structure consisting of transparent conductive oxide (TCO) glass/$TiO_2$ nanofilms as photoanodes, electrolyte, and platinum counter electrodes. The cis-diisothiocyanato-bis (4,4'-dicarboxylic acid-2,2'-bipyridine) ruthenium (II) complex (N3 dye) was used in the fabrication. The fabrication method was as follows.

$TiO_2$ P25 was added to prepare a pure $TiO_2$ slurry (10 wt%) by adding tert-butanol and deionized water (D.I. water) in a ratio of 2:1. Then, AgNWs were added at different concentrations (0.01, 0.03, 0.05, 0.07, 0.09, and 0.11 wt%). Electrodes were prepared by depositing a layer of platinum (Pt) of 10 nm thickness onto indium tin oxide (ITO) transparent conductive glass using an electroplating method at 10 mA for 40 s. In this study, Pt was used owing to its excellent catalytic activity and corrosion resistance. We used an electron beam evaporation system to deposit a Pt thin film at 10 mA for 45 s to obtain the conductive surface of ITO thinner than 6–7 nm. Pt layers serve as the cathodes and act as the catalyst for the $I^-/I_3^-$ redox couple. Additionally, the Pt layer reflects incident light to the working electrode for repeated excitations.

To prepare the composite film of AgNWs and $TiO_2$, the AgNW/$TiO_2$ composite and pure $TiO_2$ pastes were coated as the composite film onto the ITO substrates by a doctor blade method. This was repeated 3 to 5 times until the desired film thickness was obtained. After drying, the coated ITO substrate was embossed with a pressure of 20 kg/cm² for 60 s. Then, a working area of 0.25 $cm^2$ was created by removing excess coatings. The coated ITO substrates were heated at 150 ℃ for 90 min and then at 300 ℃ for 30 min for annealing.

Next, the N3 dye was prepared and the working electrode was sensitized. The dye solution was prepared by mixing tert-butanol and acetonitrile in a concentration of $3 \times 10^{-4}$ M. N3 powder was added to the mixed solution and sonicated for 2 h. The annealed ITO was soaked in the N3 dye solution in an oven at 45 ℃ for 2 h to enhance the sensitization of the electrode. Afterward, the electrode was rinsed with acetonitrile to remove excess dye and wiped with alcohol to clean the glass outside the working area. Finally, the sensitized working electrode was dried before encapsulation. The electrolyte was prepared by mixing 0.05 M iodine ($I_2$), 0.1 M lithium iodide (LiI), and 1 M 1,2-dimethyl-3-propylimidazolium iodide (DMPII). The mixture was added with 3-methoxypropionitrile (3MPN) and mixed thoroughly using an ultrasonic homogenizer.

Figure 1 shows the stack packaging of DSSCs.

(1) A small hole was drilled in the nonconductive side of the Pt cathode for electrolyte injection.
(2) A polymer thermoplastic spacer was stacked in a hollow area of $0.6 \times 0.6$ $cm^2$ of the sensitized electrode.
(3) To seal the counter and working electrodes, pressure was exerted on them at 100 ℃.
(4) A syringe was used to inject the electrolyte into the holes on the Pt cathode to displace air and fill the space.

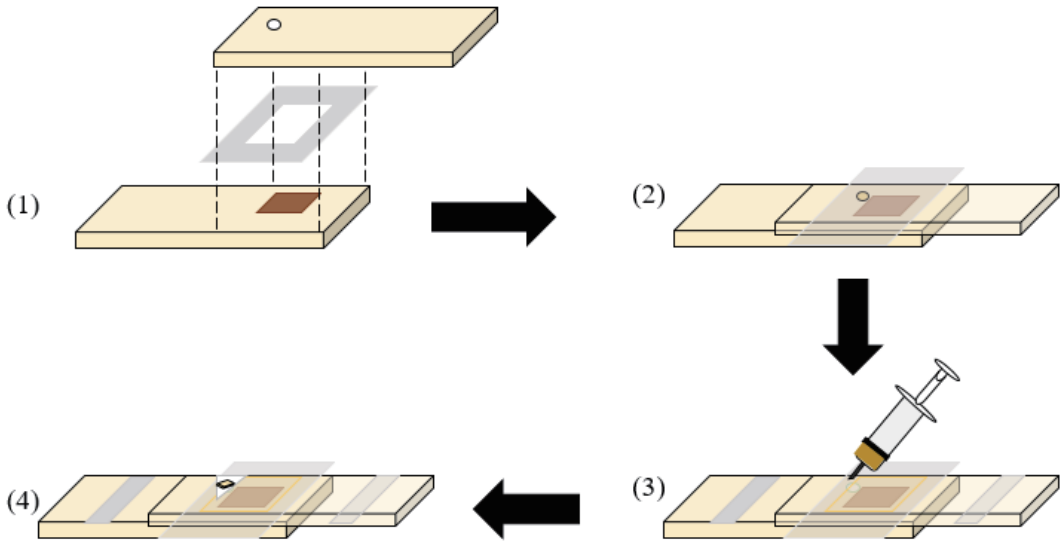


Fig. 1. (Color online) Stack packaging of DSSCs.

The holes were with small thermoplastic spacers and small glass covers to prevent evaporation and leakage. Silver paste was applied on the conductive surfaces at both ends of the electrodes, which were then dried at room temperature.

### 2.2 Measurement methods

We used the JSM-7500F cold cathode field emission scanning electron microscope (JEOL, Japan). An X-ray energy-dispersive spectrometer (EDS) was used for the qualitative and quantitative analysis of micro-elements. A Tianfeng Hydraulic TCP-3 press was used to make the photoanode surface dense and thin to increase dye adsorption and enhance the PCE of the DSSCs. The voltage–current ($J$–$V$) curves of the DSSCs were drawn using the SAN-EI Electric XES-40S1 Class A solar simulator that uses a xenon lamp as its light source. Its light path was adjusted using multilayer filters and reflectors as part of the wavelength intensity calibration method. The light source was adjusted to 1210 W/m² using a photodetector, and results and graphs were outputted using a Keithley 2400. The parameters of the $J$–$V$ curves were as follows.

(1) Open-circuit voltage ($V_{OC}$): The voltage across the positive and negative terminals of the solar cell in an open-circuit state is referred to as $V_{OC}$. When the shunt resistance ($R_{sh}$) is not considered, $V_{OC}$ decreases. A larger $R_{sh}$ results in a greater voltage division, thus increasing $V_{OC}$.

(2) Short-circuit current density ($J_{SC}$): The current across the positive and negative terminals when the solar cell is in a short-circuit state is defined as $J_{SC}$. The density of this current is known as the short-circuit current density.

(3) Fill factor ($FF$): The ratio of the maximum power output density to the product of $J_{SC}$ and $V_{OC}$ is defined as $FF$. The maximum value is 100%, which indicates that the output power under illumination is ideal. When the cell approaches the ideal diode, the angle of the $J$–$V$ curve becomes 90°, resulting in the highest $FF$ (1).

$$FF = \frac{P_{max}}{J_{SC} \times V_{OC}} \times 100\% \tag{1}$$

(4) Maximum power ($P_{max}$): Under light, the product of current density and voltage at a specific operating point gives the output power. Among the points on the curve, the maximum output power density $P_{max}$ is found at the working point defined by $V_{max}$ on the $x$-axis and $J_{max}$ on the $y$-axis.

(5) PCE ($\eta$): The ratio of the maximum output power of the solar cell to the incident light power is $\eta$. $\eta$ is calculated by multiplying the current at each voltage with the corresponding voltage in the curve [Eq. (2)]. $P_{inc}$ represents the incident light intensity, which is 100 mW/cm².

$$\eta(\%) = \frac{P_{max}\left(\mathrm{mW}/\mathrm{cm}^2\right)}{P_{inc}\left(\mathrm{mW}/\mathrm{cm}^2\right)} = \frac{J_{SC}\left(\mathrm{mA}/\mathrm{cm}^2\right) \times V_{OC}(\mathrm{mV}) \times FF}{P_{inc}\left(\mathrm{mW}/\mathrm{cm}^2\right)} \times 100(\%) \tag{2}$$

## 3. Results and Discussion

Figure 2(a) shows the composite film of AgNWs with $TiO_2$ nanoparticles. The AgNWs had a diameter of 90 nm and a length of 60 μm. The thickness of the composite film of $TiO_2$ and AgNWs on ITO is important as it affects the PCE of DSSCs. The thicker the composite film, the more dye is adsorbed. A thick composite film lengthens the electron transport path, thereby reducing the electron transfer rate and PSE. In the experiment, the film thickness was adjusted to 10 μm using a hydraulic press. Figure 2(b) shows a cross-sectional view of the composite film of 10.2 μm thickness. The weight ratios of the elements in the composite film were determined

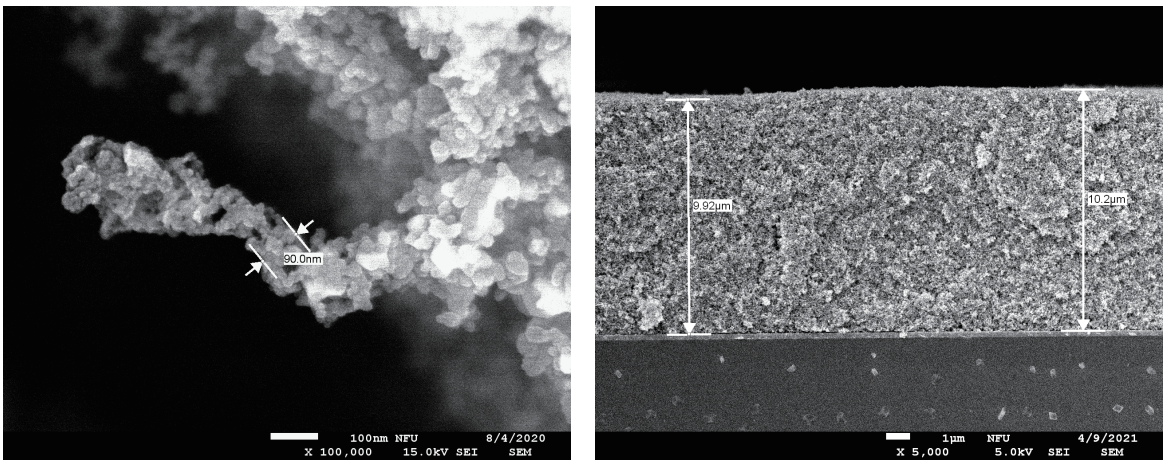


(a) (b)

Fig. 2. (a) Composite film comprising AgNWs and $TiO_2$ and (b) cross-sectional view of composite film.

using the single-point elemental analysis method of EDS. The ratios of Ti, O, and Ag were 50.94, 47.80, and 1.26 wt%, respectively.

We investigated how the concentration of AgNWs affects the performance of the DSSCs. The concentrations of AgNWs added to the composite films were 0, 0.01, 0.03, 0.05, 0.07, 0.09, and 0.11 wt%. Figure 3 shows the J–V curves of the DSSCs fabricated with AgNWs at various concentrations. The DSSC with 0.05 wt% AgNWs exhibited the highest Voc, Jsc, and FF, and the PCE was 4.14%. The efficiency was 0.6% higher than that of the DSSC without AgNWs (0 wt%). The efficiency enhancement with 0.05 wt% AgNWs was attributed to the LSPR, which generates a strong electromagnetic field due to the excitation of the molecules by light and enhances light absorption and charge separation. However, when the AgNW concentration increased beyond 0.05 wt%, the efficiency, Voc, Jsc, and FF gradually declined. Such declines were caused by a reduction in dye adsorption to the $TiO_2$ photoanode, as excess AgNWs fill the pores in the $TiO_2$ film, thereby impeding the diffusion rate of the electrolyte into the composite film. The filled pores led to the decreased electron transport and performance of the DSSCs.

Table 1 shows the Nyquist plots of the DSSCs with AgNWs at various concentrations, which were drawn using the results of electrochemical impedance spectroscopy (EIS). The series

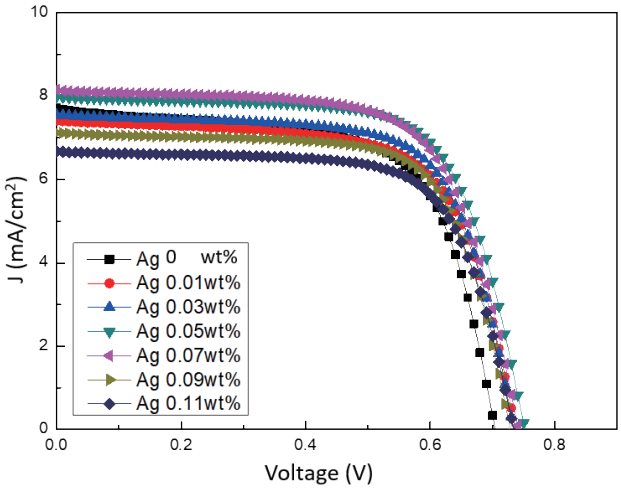


Fig. 3. (Color online) *J–V* curves of DSSCs with AgNWs (Ag: AgNW) at various concentrations.

Table 1
Parameters of DSSCs with AgNWs at various concentrations.

| AgNW concentration (wt%) | Efficiency (%) | $R_s$ | $R_{pt}$ | $R_k$ | $R_D$ | $K_{eff}$ ($s^{-1}$) | $\tau_{eff}$ (ms) |
|---|---|---|---|---|---|---|---|
| 0 | 3.54 | 13.51 | 2.7 | 17.72 | 4.40 | 32.77 | 30.51 |
| 0.01 | 3.68 | 15.17 | 2.2 | 21.86 | 2.29 | 25.31 | 39.51 |
| 0.03 | 3.82 | 14.79 | 2.6 | 25.13 | 4.70 | 32.77 | 30.51 |
| 0.05 | 4.14 | 12.88 | 2.0 | 17.19 | 3.05 | 32.77 | 30.51 |
| 0.07 | 4.07 | 13.55 | 4.4 | 24.39 | 3.29 | 25.31 | 39.51 |
| 0.09 | 3.62 | 14.95 | 2.6 | 24.31 | 2.72 | 32.77 | 30.51 |
| 0.11 | 3.41 | 15.68 | 2.8 | 24.79 | 4.92 | 25.31 | 39.51 |

resistance $R_s$ was affected by the conductivity of the glass substrate. The charge transfer resistance at the counter electrode/electrolyte interface ($R_{pt}$) is represented by the first semicircle in the high-frequency region, while the impedance at the photoelectrode/dye interface ($R_k$) is depicted by the second semicircle in the mid-frequency region. The diffusion impedance within the electrolyte ($R_D$) is illustrated by the third semicircle in the low-frequency region. The resistance ($R_k$) also indicates the recombination impedance of electrons and holes, where a higher resistance signifies more recombination. The effective rate constant of electron recombination ($K_{eff}$) is inversely related to the electron lifetime ($\tau_{eff}$); a higher $K_{eff}$ indicates a higher recombination rate and a shorter electron lifetime.

Figure 4 illustrates the incident photon-to-current efficiency (IPCE) of the DSSCs with AgNWs at various concentrations. IPCE increased from the wavelengths of 400 to 550 nm. The highest IPCEs of the DSSCs with AgNWs at various concentrations were observed between 520 and 540 nm. The highest IPCE was observed for the DSSC with 0.05 wt% AgNWs. This result indicates that 0.05 wt% AgNWs enabled the DSSC to have the optimal conversion of photons to electrical current and maximized light absorption and scattering as the morphology and distribution of AgNWs became optimal for light conversion. The prominent peak in the IPCE spectrum shows that AgNWs contributed to the increase in the performance of the DSSC at the wavelengths from 520 to 540 nm due to the LSPR that enhances the electromagnetic field around the nanowires. The exact mechanism can be elucidated through subsequent studies, the results of which provide how to optimize AgNW-based solar cells or photodetectors and a reference for effective designs to lower production costs but increase the performance of solar cells.

Figure 5 shows the absorbance of the DSSCs at different wavelengths in their sensitized but nonencapsulated states. The absorbance of the working electrode was measured. At 0.05 wt% AgNWs, the dispersion effect of the working electrode became optimal for light conversion

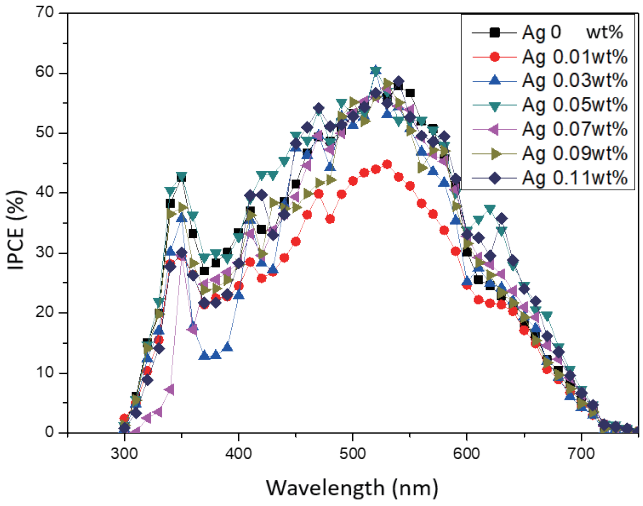


Fig. 4. (Color online) IPCE of DSSCs with AgNWs (Ag: AgNW) at various concentrations.

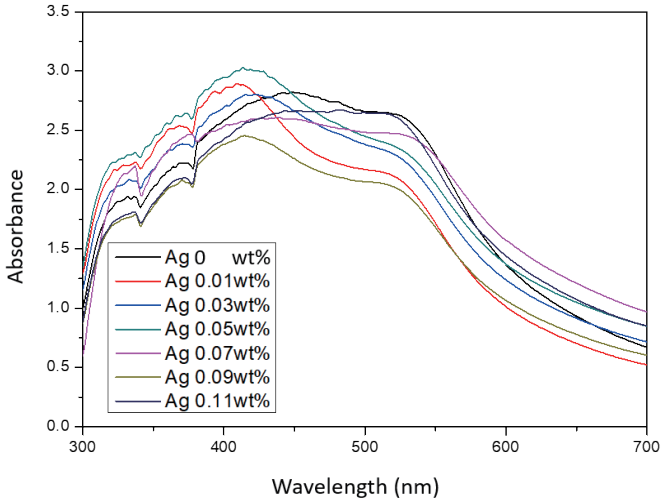


Fig. 5. (Color online) Absorbance of DSSCs with AgNWs (Ag: AgNW) at various concentrations.

owing to the uniform distribution of $TiO_2$ and increased dye adsorption. In general, the absorption peak of the N3 dye is observed at 538 nm. The experiment result showed that absorption decreased beyond 538 nm for all DSSCs with AgNWs at various concentrations. Such a decrease in absorption is attributed to insufficient light absorption at wavelengths longer than 538 nm. The addition of AgNWs facilitates the dispersion of $TiO_2$ and the increase in dye adsorption, which improves the performance of DSSCs. The optimal concentration of AgNWs for improving the performance of DSSCs was 0.05 wt% at 538 nm. Beyond this concentration, the dye exhibits limited light absorption. This suggests that while the AgNWs improve dispersion and adsorption, it is still necessary to study how to enhance light absorption across the entire spectrum of light for better DSSC performance.

## 4. Conclusions

We investigated the impact of AgNWs on the performance of DSSCs. AgNWs of 0, 0.01, 0.03, 0.05, 0.07, 0.09, and 0.11 wt% with $TiO_2$ were coated to the ITO of the DSSCs, and their ability of converting light to electric energy was measured. Adding 0.05 wt% AgNWs resulted in the highest PCE of 4.14% and the highest IPCE and absorbance. The highest open-circuit voltage of 0.75 V and $J_{sc}$ of 8.14 mA/cm² were also obtained from the DSSC with 0.05 wt% AgNWs. The best electron lifetime, the lowest electron–hole recombination rate, and the highest specific surface area were also observed along with the lowest $R_s$, $R_{pt}$, $R_k$, and $K_{eff}$. It was confirmed that adding an optimal amount of AgNWs effectively enhanced the photovoltaic efficiency of the DSSC. The performance enhancement is attributed to increased ductility, thermal conductivity, electrical conductivity, and reflectivity, and reduced resistance due to the properties of Ag. At higher AgNW concentrations, the conductivity between the electrode and the electrolyte decreased as the pores of the composite film were filled with Ag. Then, $R_D$ increased, ultimately decreasing the efficiency of the DSSC. Such results can be used to develop more efficient DSSCs using AgNWs.

## References


1 U. Bach, D. Lupo, P. Comte, J. E. Moser, F. Weissörtel, J. Salbeck, H. Spreitzer, and M. Grätzel: Nature **395** (1998) 583. https://doi.org/10.1038/26936
2 H. Michaels, M. Rinderle, R. Freitag, I. Benesperi, T. Edvinsson, R. Socher, A. Gagliardi, and M. Freitag: Chem. Sci. **11** (2020) 2895. https://doi.org/10.1039/c9sc06145b
3 M. Kokkonen, P. Talebi, J. Zhou, S. Asgari, S. A. Soomro, F. Elsehrawy, J. Halme, S. Ahmad, A. Hagfeldt, and S. G. Hashmi: J. Mater. Chem. A **9** (2021) 10527. https://doi.org/10.1039/d1ta00690h
4 Rahmadwati, S. N. Sari, E. Maulana, and A. Sabarudin: Indones. J. Electr. Eng. Comput. Sci. **12** (2018) 685. https://doi.org/10.11591/ijeecs.v12.i2.pp685-690
5 M. Kokkonen, P. Talebi, J. Zhou, S. Asgari, S. A. Soomro, F. Elsehrawy, J. Halme, S. Ahmad, A. Hagfeldt, and S. G. Hashmi: J. Mater. Chem. A **9** (2021) 10527. https://doi.org/10.1039/D1TA00690H
6 A. Aslam, U. Mehmood, M. H. Arshad, A. Ishfaq, J. Zaheer, A. U. H. Khan, and M. Sufyan: Sol. Energy **207** (2020) 874. https://doi.org/10.1016/j.solener.2020.07.029
7 B. D. Choudhury, C. Lin, S. M. A. Z. Shawon, J. Soliz Martinez, H. Huq, and M. J. Uddin: Sci. Rep. **11** (2021) 7552. https://doi.org/10.1038/s41598-021-87123-z
8 P. N. Prasad: Nanophotonics (John Wiley & Sons, New Jersey, 2004) Chap. 1. https://doi.org/10.1002/0471670251.ch10